

---

# Gd-EOB-DTPA-Enhanced MRI Combined with ALBI Score and AFP for Predicting Histologic Grade in Hepatocellular Carcinoma: A Multicenter Study from Vietnam

---

[Hung Nguyen Van](#)\*, Luu Vu Dang, Anh Nguyen The, Long Nguyen Cong, Khang Le Van, Trung Nguyen Ngoc, [Minh Vu Le](#), Hoi Nguyen Ham

Posted Date: 7 May 2026

doi: 10.20944/preprints202605.0460.v1

Keywords: hepatocellular carcinoma; Gd-EOB-DTPA; magnetic resonance imaging; histologic grade; Edmondson-Steiner; ALBI score; alpha-fetoprotein; hepatobiliary phase



Preprints.org is a free multidisciplinary platform providing preprint service that is dedicated to making early versions of research outputs permanently available and citable. Preprints posted at Preprints.org appear in Web of Science, Crossref, Google Scholar, Scilit, Europe PMC, OpenAlex.

Copyright: This open access article is published under a [Creative Commons CC BY 4.0 license](#), which permit the free download, distribution, and reuse, provided that the author and preprint are cited in any reuse.

Disclaimer/Publisher's Note: The statements, opinions, and data contained in all publications are solely those of the individual author(s) and contributor(s) and not of MDPI and/or the editor(s). MDPI and/or the editor(s) disclaim responsibility for any injury to people or property resulting from any ideas, methods, instructions, or products referred to in the content.

Article

# Gd-EOB-DTPA-Enhanced MRI Combined with ALBI Score and AFP for Predicting Histologic Grade in Hepatocellular Carcinoma: A Multicenter Study from Vietnam

Hung Nguyen Van <sup>1,2,\*</sup>, Luu Vu Dang <sup>1,3</sup>, Anh Nguyen The <sup>4</sup>, Long Nguyen Cong <sup>3</sup>,  
Khang Le Van <sup>3</sup>, Trung Nguyen Ngoc <sup>2</sup>, Minh Vu Le <sup>4</sup> and Hoi Nguyen Ham <sup>3</sup>

<sup>1</sup> Hanoi Medical University, Hanoi, Vietnam

<sup>2</sup> Department of Diagnostic Imaging, Thai Binh University of Medicine and Pharmacy, Thai Binh, Vietnam

<sup>3</sup> Bach Mai Hospital, Hanoi, Vietnam

<sup>4</sup> K Hospital, Hanoi, Vietnam

\* Correspondence: drhungytb@gmail.com; Tel.: +84 354050686

## Abstract

**Objectives:** Histologic grade is an important prognostic factor in hepatocellular carcinoma (HCC). Gd-EOB-DTPA-enhanced MRI may provide noninvasive imaging markers related to tumour differentiation. This study aimed to evaluate the association of Gd-EOB-DTPA-enhanced MRI features, together with the albumin-bilirubin (ALBI) score and alpha-fetoprotein (AFP), with HCC histologic grade and to assess the performance of combined predictive models. **Methods:** Methods: In this prospective cross-sectional study, 75 patients (mean age, 56.4 years; 66 men) with 88 histopathologically confirmed HCC lesions were enrolled. Patients were classified into well-differentiated (grade I–II, n = 24) and poorly differentiated (grade III–IV, n = 51) groups according to the Edmondson–Steiner system. MRI was performed on a 1.5-T scanner and included T1-weighted in-phase/opposed-phase imaging, T2-weighted imaging, diffusion-weighted imaging, and dynamic Gd-EOB-DTPA-enhanced sequences, including arterial, portal venous, transitional, and 20-min hepatobiliary phases. Two radiologists, blinded to pathology, assessed predefined imaging features, and the lesion-to-liver ratio (LLR) was measured. Group comparisons were performed using Student's t-test, the Mann–Whitney U test, and the chi-square or Fisher's exact test, followed by multivariable logistic regression and ROC analysis with 500 bootstrap resamples. **Results:** Compared with well-differentiated HCC, poorly differentiated HCC showed a higher frequency of peritumoral hepatobiliary phase (HBP) hypointensity (62.7% vs. 4.2%,  $p < 0.001$ ) and peritumoral arterial hyperintensity (39.2% vs. 0%,  $p < 0.001$ ). In multivariable analysis, peritumoral HBP hypointensity remained independently associated with poorly differentiated HCC (OR = 30.89,  $p = 0.002$ ). The 2-parameter MRI model, including peritumoral HBP hypointensity and HBP tumour signal, yielded an AUC of 0.84. The combined MRI + ALBI + AFP model showed the highest discriminative performance, with an AUC of 0.87 and an accuracy of 78.7%. **Conclusions:** Conclusions: Gd-EOB-DTPA-enhanced MRI features, particularly peritumoral HBP hypointensity, were associated with high histologic grade in HCC. In this cohort, combining MRI features with ALBI grade and AFP yielded higher discriminative performance than the MRI-only model. These findings may support preoperative histologic risk stratification, although external validation is required.

**Keywords:** hepatocellular carcinoma; Gd-EOB-DTPA; magnetic resonance imaging; histologic grade; Edmondson–Steiner; ALBI score; alpha-fetoprotein; hepatobiliary phase

## 1. Introduction

Hepatocellular carcinoma (HCC) is the sixth most common cancer worldwide and the third leading cause of cancer-related death, with an estimated 866,000 new cases and 758,000 deaths in 2022 [1]. In Vietnam, liver cancer ranks second in incidence (24,502 cases, 13.6%) and first in cancer-related mortality (23,333 deaths, 19.4%) [1], representing a major public health burden due to the high prevalence of chronic hepatitis B virus (HBV) and hepatitis C virus (HCV) infection [2]. In this context, pre-treatment prognostic assessment depends not only on tumour size or number, but also, importantly, on tumour biology, particularly histologic grade [3].

The Edmondson-Steiner (ES) classification is the most widely used histologic grading system for HCC [4], categorising tumours from grade I (well differentiated) to grade IV (undifferentiated). Poorly differentiated HCC (grade III[-]IV) has been associated with a higher rate of microvascular invasion (MVI), earlier recurrence after curative treatment, and poorer overall survival [5]. Therefore, accurate preoperative prediction of histologic grade is of considerable clinical relevance.

Gadoxetic acid (Gd-EOB-DTPA, Primovist®) is a hepatocyte-specific MRI contrast agent that provides information on both dynamic contrast-enhanced phases and the hepatobiliary phase (HBP) [6]. During the HBP, Gd-EOB-DTPA is taken up through the OATP1B3 transporter, allowing indirect assessment of hepatocellular function. Poorly differentiated HCCs exhibit reduced or absent OATP expression, resulting in characteristic hypointensity on HBP images, and the degree of signal reduction reflects the level of OATP1B3 expression in tumour cells [7]. Several studies have shown that peritumoral HBP hypointensity, peritumoral arterial hyperintensity, and LLR are associated with histologic grade and microvascular invasion [7,8].

In addition to imaging findings, AFP has been investigated as a predictor of HCC differentiation and has been incorporated into nomograms for preoperative prediction of histologic grade [9]. AFP levels tend to increase with loss of differentiation, reflecting the biological link between AFP expression and tumour aggressiveness [10]. The ALBI score, which is derived from serum albumin and bilirubin, provides an objective assessment of hepatic reserve and has been associated with tumour behaviour through its relationship with early postoperative recurrence [11]. However, the combined value of Gd-EOB-DTPA-enhanced MRI, the ALBI score, and AFP for predicting HCC histologic grade remains incompletely defined, and no Vietnamese study has yet evaluated predictive models for HCC histologic grading. Therefore, we conducted this study to investigate the association of Gd-EOB-DTPA MRI features, the ALBI score, and AFP with HCC histologic grade, and to evaluate the diagnostic performance of individual parameters and combined models for predicting poorly differentiated HCC (grade III[-]IV).

## 2. Materials and Methods

### 2.1. Study Population

This cross-sectional analytical study was conducted at Bach Mai Hospital and K Hospital. Patients with HCC who underwent Gd-EOB-DTPA-enhanced MRI between May 2025 and January 2026 were prospectively enrolled.

Inclusion criteria: (1) histopathologically confirmed HCC based on surgical specimens; (2) Gd-EOB-DTPA-enhanced MRI performed within 4 weeks before tissue sampling; (3) complete clinical, imaging, and laboratory data.

Exclusion criteria: (1) prior treatment before MRI; (2) inadequate image quality; (3) combined hepatocellular-cholangiocarcinoma.

A total of 75 patients with 88 tumors were included; however, inferential analyses focused on the index lesion of each patient.

## 2.2. Study Methods

### 2.2.1. MRI Acquisition

MRI was performed on a 1.5-T scanner. The imaging protocol included in-phase/opposed-phase T1-weighted imaging, T2-weighted imaging, diffusion-weighted imaging (DWI), and dynamic contrast-enhanced imaging. Gd-EOB-DTPA (Primovist®) was administered at a dose of 0.025 mmol/kg at a rate of 1 mL/s, followed by a 20-mL saline flush. Imaging phases included arterial phase (20[-]35 s), portal venous phase (60[-]80 s), transitional phase (3 min), and hepatobiliary phase (20 min) [12].

### 2.2.2. Image Analysis

Two radiologists with more than 5 years of experience independently reviewed all MRI studies while blinded to histopathologic results. The following imaging features were assessed: APHE, washout, and capsule appearance according to LI-RADS 2018 criteria [13]; peritumoral arterial hyperintensity; peritumoral HBP hypointensity; tumour signal intensity on HBP; and the lesion-to-liver ratio (LLR), defined as the ratio of tumour signal intensity to adjacent liver parenchymal signal intensity on HBP images. Measurements were obtained using a single region of interest (ROI) placed in the central portion of the lesion, including the most hypointense area, and a corresponding ROI placed in the adjacent liver parenchyma on the same slice. Each ROI had an area of at least 1.5 cm [2]. Representative hepatobiliary-phase MRI findings and the region-of-interest (ROI)-based approach used for lesion-to-liver ratio (LLR) measurement are shown in Figure 1.

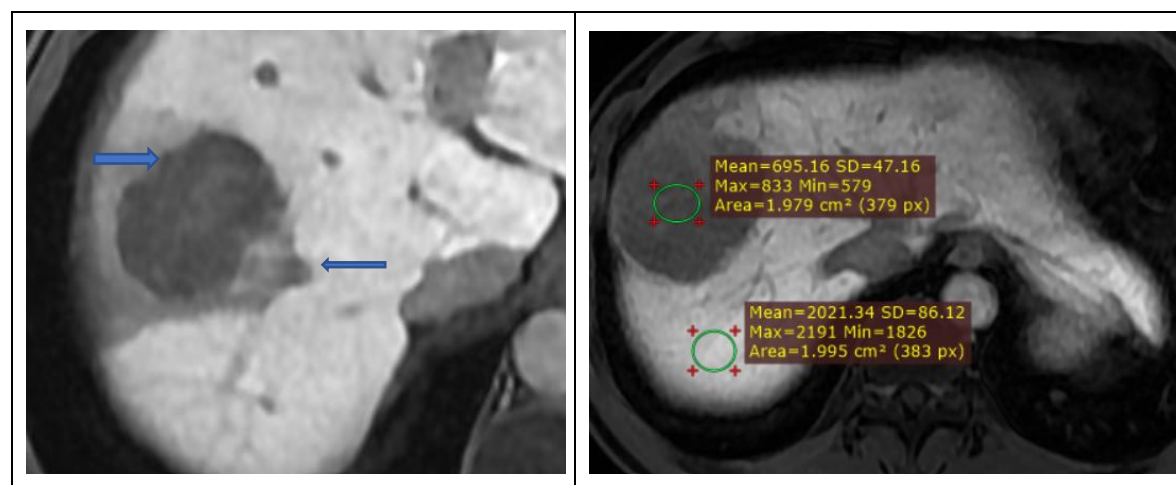


**Figure 1.** Image showing signal-reduction margins around the tumor (HBP) and how to measure the ROI of the tumor and liver parenchyma to calculate LLR in two different HCC patients with grade III E-S. A. The signal-reduction margins around the tumor (HBP) are areas of decreased signal compared to healthy liver parenchyma, but still show increased signal compared to the tumor (blue arrows). B. Illustration of measuring the signal ROI of the tumor (excluding necrotic and bleeding areas of the tumor) and healthy liver parenchyma on the same slice.

### 2.2.3. Histopathology

Histopathologic grading was performed according to the Edmondson-Steiner classification. For heterogeneous tumours, the highest histologic grade was recorded. Tumours were then categorised into two groups: well-differentiated (grades I[-]II) and poorly differentiated (grades III[-]IV).

### 2.2.4. Clinical and Biochemical Variables

Clinical and laboratory variables included age, sex, HBV/HCV status, cirrhosis, AFP level (ng/mL), bilirubin ( $\mu\text{mol/L}$ ), albumin (g/L), AST, and ALT (U/L). The ALBI score was calculated as  $\text{ALBI} = (\log_{10} \text{bilirubin} \times 0.66) + (\text{albumin} \times [-]0.085)$  [15].

ALBI grades were defined as follows: grade 1 ( $\leq [-]2.60$ ), grade 2 ( $> [-]2.60$  to  $\leq [-]1.39$ ), and grade 3 ( $> [-]1.39$ ).

### 2.2.5. Pathologic Assessment

Histopathologic findings were evaluated by a gastrointestinal/hepatobiliary pathologist with more than 5 years of experience, independently and blinded to MRI findings. Additional recorded features included true microvascular invasion (MVI), microscopic tumor size, and parenchymal fibrosis. Representative histopathologic appearances across the Edmondson–Steiner spectrum are shown in Figure 2.

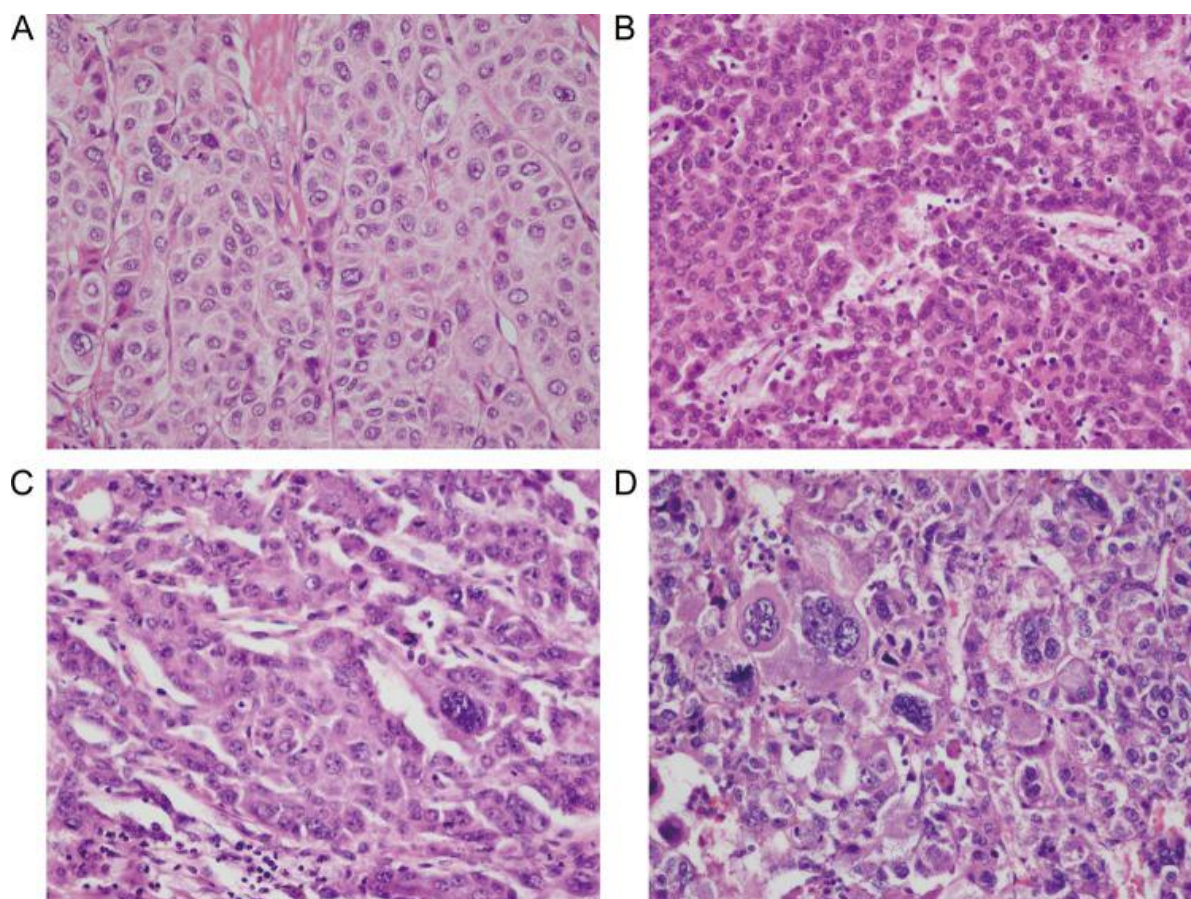


**Figure 2.** Representative histopathologic appearances of hepatocellular carcinoma across the Edmondson–Steiner spectrum. (A) Well-differentiated tumor with relatively preserved trabecular architecture and mild nuclear atypia; (B) moderately differentiated tumor with increased cellularity and nuclear irregularity; (C) poorly differentiated tumor with marked architectural distortion; (D) high-grade tumor with pronounced pleomorphism and marked atypia.

### 2.3. Statistical Analysis

Normally distributed continuous variables were expressed as mean  $\pm$  standard deviation and compared using the Student t test. Non-normally distributed variables were expressed as median (interquartile range) and compared using the Mann-Whitney U test. Categorical variables were expressed as frequency (%) and compared using the chi-square test or Fisher's exact test. Variables with  $p < 0.10$  on univariable analysis were entered into multivariable logistic regression. ROC analysis was performed to calculate the AUC, sensitivity, specificity, positive predictive value (PPV), negative predictive value (NPV), and accuracy. Bootstrap resampling was performed 500 times. A  $p$ -value  $< 0.05$  was considered statistically significant. Statistical analyses were conducted using SPSS version 27.0.

#### 2.4. Ethical Considerations

This study was conducted in accordance with the Declaration of Helsinki and was approved by the Biomedical Ethics Committee of Bach Mai Hospital (IRB00009695). Patients and their families were thoroughly informed about the study objectives and procedures. Participants were free to withdraw from the study at any time.

### 3. Results

A total of 75 patients with HCC were included: 24 (32.0%) with well-differentiated tumors (grade I[-]II) and 51 (68.0%) with poorly differentiated tumors (grade III[-]IV).

**Table 1.** Clinical and biochemical characteristics according to ES group (n=75).

Variable	Grade I–II (n=24)	Grade III–IV (n=51)	p-value
Demographic characteristics, mean ± SD			
Age (years)	54.46 ± 12.65	57.35 ± 10.64	0.39
Sex, n (%)			
Male	22 (91.7)	44 (86.3)	0.77
Female	2 (8.3)	7 (13.7)	0.77
Medical history and risk factors, n (%)			
Hepatitis C	3 (12.5)	7 (13.7)	0.90
Hepatitis B	20 (83.3)	40 (78.4)	0.76
Underlying cirrhosis	8 (33.3)	13 (25.5)	0.58
Biochemical markers, mean ± SD or median (IQR)			
AFP (ng/mL)	9.2 (4.6–110.2)	42.4 (10.1–361.2)	0.10
Bilirubin (μmol/L)	13.02 ± 4.75	11.90 ± 5.87	0.28
Albumin (g/L)	43.92 ± 2.57	41.72 ± 3.06	0.002
Liver functional reserve			
ALBI score, mean ± SD	-3.01 ± 0.20	-2.90 ± 0.36	0.11
ALBI grade, n (%)			
Grade 1	24 (100)	43 (84.3)	0.05
Grade 2–3	0 (0.0)	8 (15.7)	

SD: standard deviation; IQR: interquartile range.

Patients with poorly differentiated HCC according to the Edmondson-Steiner classification (ES III[-]IV) had significantly lower serum albumin levels than those with ES I[-]II tumors (41.72 ± 3.06 vs 43.92 ± 2.57 g/L,  $p = 0.002$ ). The proportion of patients with ALBI grade 2[-]3 was also higher in the ES III[-]IV group, whereas age, sex, HBV/HCV status, cirrhosis, AFP, bilirubin, and the continuous ALBI score did not differ significantly between groups.

**Table 2.** Gd-EOB-DTPA MRI features according to ES group (n=75).

Imaging feature	Grade I–II (n=24)	Grade III–IV (n=51)	p-value
Tumor size			
Largest tumor diameter (mm), mean ± SD	45.88 ± 26.02	55.02 ± 24.27	0.02
Number of tumors per patient	27	61	

Tumor number, n (%)			
1 lesion	21 (87.5)	43 (84.3)	0.72
≥2 lesions	3 (12.5)	8 (15.7)	
APHE, n (%)			
Present	23 (95.8)	46 (90.2)	0.66
Absent	1 (4.2)	5 (9.8)	
Washout, n (%)			
Present	16 (66.7)	45 (88.2)	0.06
Absent	8 (33.3)	6 (11.8)	
Capsule appearance, n (%)			
Present	14 (58.3)	30 (58.8)	0.97
Absent	10 (41.7)	21 (41.2)	
Hepatobiliary phase tumor signal, n (%)			
Hypointense	7 (29.2)	36 (70.6)	0.002
Hyperintense	11 (45.8)	11 (21.6)	
Isointense / non-specific	6 (25.0)	4 (7.8)	
Tumor-to-liver signal ratio (LLR), mean ± SD	0.62 ± 0.29	0.47 ± 0.13	0.03
Peritumoral arterial hyperintensity, n (%)			
Present	0 (0.0%)	20 (39.2%)	<0.001
Absent	24 (100%)	31 (60.8%)	
Peritumoral HBP hypointensity, n (%)			
Present	1 (4.2%)	32 (62.7%)	<0.001
Absent	23 (95.8%)	19 (37.3%)	
Quantitative index			
HBP LLR, mean ± SD	0.62 ± 0.29	0.47 ± 0.13	0.03

APHE: arterial phase hyperenhancement; HBP: hepatobiliary phase; LLR: lesion-to-liver ratio. The entire cohort comprised 88 tumours on MRI; however, comparisons in this table were performed at the patient/index-lesion level.

The ES III[-]IV group showed a more aggressive imaging profile on Gd-EOB-DTPA-enhanced imaging, including larger tumour size, more frequent peritumoral arterial hyperintensity, more frequent peritumoral HBP hypointensity, a higher proportion of HBP hypointensity, and lower HBP LLR values. In contrast, tumour number, APHE, capsule appearance, and washout did not differ substantially between the two groups.

**Table 3.** Univariable logistic regression analysis for predicting high histologic grade HCC (ES III[-]IV).

Predictor	B coefficient	SE	OR	95% CI	p-value
Peritumoral HBP hypointensity					
No			1.00	Reference	<0.001
Yes	3.66	1.06	38.74	4.83–310.39	
HBP tumor signal intensity	1.15	0.37	3.16	1.52–6.54	0.002
Tumor size	0.18	0.12	1.19	0.94–1.52	0.149
HBP LLR	0.38	0.15	1.46	1.09–1.95	0.01
Elevated AFP (≥20 ng/mL)					
No			1.00	Reference	0.04

Yes	1.03	0.51	2.80	1.03–7.60	
Liver function (ALBI)					
ALBI score	1.20	0.85	3.32	0.62–17.71	0.149

In univariable analysis, peritumoral HBP hypointensity, HBP tumour signal intensity, LLR, and elevated AFP ( $\geq 20$  ng/mL) were significantly associated with high histologic grade HCC (ES III[-]IV). Among these, peritumoral HBP hypointensity showed the strongest association (OR = 38.74,  $p < 0.001$ ). In contrast, ALBI score, tumour size, and APHE did not show significant associations in the present dataset.

**Table 4.** Multivariable logistic regression analysis for predicting high histologic grade HCC (ES III[-]IV).

Predictor	B coefficient	SE	OR	95% CI	p-value
Peritumoral HBP hypointensity					
No			1.00	Reference	0.002
Yes	3.43	1.11	30.89	3.54–269.66	
HBP tumor signal intensity	0.72	0.44	2.06	0.87–4.87	0.10
Elevated AFP ( $\geq 20$ ng/mL)					
No			1.00	Reference	0.38
Yes	-0.58	0.66	0.56	0.15–2.04	
Liver function (ALBI)					
ALBI score	1.03	1.01	2.81	0.39–20.32	0.31
Constant	2.36	3.03			0.44

Multivariable regression was performed on the index lesion of 75 patients; the entire cohort comprised 88 tumors on MRI. In the multivariable model, peritumoral HBP hypointensity remained an independent predictor of high histologic grade HCC (ES III[-]IV) (OR = 30.89, 95% CI: 3.54[-]269.66,  $p = 0.002$ ). HBP tumor signal intensity showed a trend in the same direction but did not reach statistical significance ( $p = 0.10$ ), while elevated AFP and ALBI score were not independently associated.

The preliminary total-score formula was as follows: Total score =  $100 \times$  (peritumoral HBP hypointensity) +  $21 \times$  (HBP tumor signal level) +  $17 \times$  (AFP < 20 ng/mL) +  $30 \times$  (ALBI + 3.5)

where peritumoral HBP hypointensity = 1 if present, 0 if absent; HBP tumor signal level = 0, 1, or 2; AFP < 20 = 1 if AFP < 20 ng/mL, 0 if AFP  $\geq 20$  ng/mL.

**Table 5.** Diagnostic performance of individual parameters and combined models for predicting poorly differentiated HCC.

Predictive model	AUC	Se (%)	Sp (%)	PPV (%)	NPV (%)	Accuracy (%)
Individual parameters						
Tumor size (cm)	0.67	90.2	45.8	78.0	68.8	76.0
APHE	0.53	9.8	95.8	83.3	33.3	37.3
Peritumoral HBP hypointensity	0.79	62.7	95.8	97.0	54.8	73.3
HBP tumor signal intensity	0.72	70.6	70.8	83.7	53.1	70.7
Elevated AFP ( $\geq 20$ ng/mL)	0.57	76.5	37.5	72.2	42.9	64.0

ALBI grade 2-3	0.58	15.7	100	100	35.8	42.7
Combined models						
2-parameter MRI model	0.84	62.7	95.8	97.0	54.8	73.3
4-parameter combined model	0.87	74.5	87.5	92.7	61.8	78.7

AUC: area under the ROC curve; Se: sensitivity; Sp: specificity; PPV: positive predictive value; NPV: negative predictive value. 2-parameter MRI model: peritumoral HBP hypointensity + HBP tumor signal intensity. 4-parameter combined model: peritumoral HBP hypointensity + HBP tumor signal intensity + elevated AFP + ALBI grade 2[-]3.

Among the individual parameters, peritumoral HBP hypointensity showed the highest diagnostic performance (AUC = 0.79), followed by HBP tumour signal intensity (AUC = 0.72). Combining these two imaging markers yielded a 2-parameter MRI model with an AUC of 0.84. The addition of elevated AFP and ALBI grade 2[-]3 further increased the AUC to 0.87, suggesting improved discrimination for poorly differentiated HCC.

#### 4. Discussion

Our results suggest that hepatobiliary phase imaging features, particularly peritumoral HBP hypointensity and reduced tumour signal on HBP images, are associated with poorly differentiated HCC.

A notable finding of this study was the association between peritumoral HBP hypointensity and poorly differentiated HCC, with an estimated OR of 38.74. Peritumoral HBP hypointensity has been regarded as an imaging marker of microvascular invasion, reflecting the invasive biological behaviour of the tumour. The proposed mechanism is that microscopic tumour thrombi in the peritumoral portal venules reduce or obstruct portal venous flow, leading to impaired hepatocyte function and decreased uptake of Gd-EOB-DTPA in the surrounding liver tissue, thereby creating a hypointense rim relative to the adjacent liver parenchyma. The high specificity (95.8%) and PPV (97.0%) of this sign suggest that it may reflect more aggressive tumour biology, in keeping with previous reports [14,15].

The degree of hepatobiliary phase tumour hypointensity was another imaging feature associated with histologic grade (OR = 3.16,  $p = 0.002$ ), and its quantitative counterpart, LLR, also showed predictive value, possibly reflecting progressive loss of OATP1B3 expression during dedifferentiation. As HCC progresses from well-differentiated to poorly differentiated forms, the expression of hepatocyte-specific membrane transporters gradually decreases, leading to reduced uptake of Gd-EOB-DTPA [7]. The lower LLR observed in poorly differentiated HCC (0.47 vs 0.62) may therefore reflect this progressive loss of OATP1B3 expression during tumour dedifferentiation. LLR also offers the advantage of being an objective measurement that is less dependent on scanner-specific signal intensity, as it represents a relative ratio between tumour and background liver signal on the same image slice.

Peritumoral arterial hyperintensity was observed only in the poorly differentiated group (39.2% vs. 0%,  $p < 0.001$ ) in univariable analysis but did not remain significant in the multivariable model ( $p = 0.42$ ), possibly because of collinearity with peritumoral HBP hypointensity, as both features have been linked to microvascular invasion [14]. Poorly differentiated HCC also had a larger tumour size ( $p = 0.02$ ), although tumour size was not independently associated in the multivariable model, suggesting that it may function more as a surrogate marker than as a direct indicator of tumour aggressiveness. Washout on the portal venous phase showed a non-significant trend toward being

more frequent in poorly differentiated tumours ( $p=0.06$ ), consistent with decreased portal venous supply and increased arterial perfusion in more aggressive lesions [12].

The ALBI score is an objective model based on two routine blood biomarkers, albumin and bilirubin. Although it was not independently associated with histologic grade in the multivariable model, lower albumin levels were observed in the poorly differentiated group ( $p = 0.002$ ), which may indicate a relationship between hepatic functional reserve and tumour behaviour. This may be explained by the fact that poorly differentiated tumours tend to occur in patients with more advanced underlying liver disease, resulting in reduced albumin synthesis. The relationship between a higher ALBI score and recurrence after surgery has also been reported by Demirtas et al. [11]. who identified ALBI as a predictor of survival, recurrence, and post-hepatectomy liver failure. Zhou et al. (2023)[9] also incorporated ALBI into a nomogram to predict histologic grade, using it as an objective alternative to the Child-Pugh classification for assessing liver functional reserve. Overall, ALBI is currently used mainly as a marker of liver function and prognosis.

In the present study, AFP tended to be higher in the poorly differentiated group (median 42.4 vs 9.2 ng/mL) and was statistically significant ( $p=0.04$ ). In univariable analysis, AFP had predictive value; however, its AUC was modest, remaining only moderate. Previous studies have also reported an association between AFP level and histologic grade in HCC. In a large-scale study of 78,743 HCC patients from the SEER database, Bai et al. [16]. showed that positive AFP at diagnosis was an independent risk factor for higher histologic grade (OR = 2.559, 95% CI: 2.075[-]3.157,  $p < 0.001$ ). This study also demonstrated that AFP was an independent predictor of mortality in both surgical and non-surgical groups. Similarly, Edoo et al. [17]. reported that mean AFP levels were highest in poorly differentiated HCC, confirming a positive relationship between AFP level and degree of dedifferentiation.

Recently, several preoperative prediction models for HCC histologic grade have been published using combined imaging and biomarker data. Zhou et al. [9]. developed a nomogram for predicting ES III[-]IV in 240 HCC patients, integrating AFP, des- $\gamma$ -carboxy prothrombin, HBsAg, HCV antibody, ALRI, and macrovascular invasion on imaging. In that study, AFP and DCP were identified as independent predictors of ES III[-]IV, and the proportion of patients with both AFP and DCP positivity was significantly higher in the MVI and ES III[-]IV groups. Compared with the model reported by Zhou et al., our study additionally evaluated hepatobiliary phase-specific imaging features, including peritumoral HBP hypointensity and reduced HBP tumour signal, which are not available on CT or extracellular contrast-enhanced MRI [19].

In the field of radiomics, Yan et al. [18]. developed a multiphase Gd-EOB-DTPA-enhanced MRI radiomics signature to predict HCC histologic grade in 405 patients, with AFP as an important input variable alongside radiomic features. Similarly, Mao et al. (2022) [19] constructed an artificial neural network (ANN) model combining the radiomic features of Gd-EOB-DTPA radiometric imaging in the hepatobiliary phase with AFP, achieving an AUC of 0.941 for differentiating high and low histological grade HCC. In that study, the AFP-integrated ANN-HBP model outperformed the logistic regression model (AUC 0.941 vs. 0.819;  $p = 0.001$ ), suggesting that AFP may add discriminative value when combined with hepatobiliary phase imaging features. This is broadly consistent with the present findings, in which AFP alone showed modest discriminative ability, whereas the combined model yielded an AUC of 0.87 and an accuracy of 78.7%. He et al. [20]. used Gd-EOB-DTPA-enhanced T1 mapping combined with ADC values from DWI. They found that  $\Delta T1$  decreased progressively as histologic differentiation worsened, and the combined model achieved an AUC of 0.811. Overall, the AUC range of 0.84–0.87 in our study is comparable to that reported in recent studies and suggests that combining conventional imaging features with AFP and ALBI may be feasible in settings where advanced radiomics infrastructure is not routinely available.

Although ALBI was not independently associated with histologic grade in multivariable analysis, inclusion of ALBI together with peritumoral HBP hypointensity, tumour HBP signal, and AFP produced a combined model with an AUC of 0.87, a specificity of 87.5%, and an accuracy of 78.7%, which was higher than that of the 2-parameter MRI model alone (AUC 0.84). This suggests

that combining imaging features with laboratory variables may improve model performance. This is particularly relevant in routine clinical practice because ALBI is derived from albumin and total bilirubin, which are inexpensive, widely available laboratory tests, and AFP is routinely performed. Accordingly, this integrated model may be relevant to preoperative assessment workflows, particularly in settings with variable resource availability; however, further validation is needed. Combined models showed better discriminative performance than individual parameters in this dataset. The 2-parameter MRI model achieved an AUC of 0.84 and a specificity of 95.8%. The integrated MRI + ALBI + AFP model yielded an AUC of 0.87 and an accuracy of 78.7%, suggesting that adding simple laboratory variables to a focused MRI model may improve discrimination. Preoperative identification of high histologic grade HCC may support preoperative risk stratification and may be relevant to treatment planning and follow-up strategies [21,22].

This study has several limitations. First, the sample size was relatively small ( $n=75$ ), leading to a wide confidence interval for the OR of peritumoral HBP hypointensity (4.83[-310.40]). Second, the distribution between groups was unbalanced, and the study population consisted predominantly of surgically treated HBV-related HCC. Larger prospective multicenter studies with external validation are needed to confirm these findings and to better define their clinical applicability.

## 5. Conclusions

Gd-EOB-DTPA-enhanced MRI features, particularly peritumoral hepatobiliary phase hypointensity and reduced tumour signal on HBP images, were associated with high histologic grade in HCC. Among the evaluated imaging features, peritumoral HBP hypointensity showed the largest estimated independent association in the multivariable model. The combined models showed moderate-to-good discriminative performance, with AUC values ranging from 0.84 to 0.87 in this cohort, and may support preoperative histologic risk stratification; however, external validation is required before broader clinical application.

**Author Contributions:** NVH: Conceptualization, study design, data acquisition, imaging evaluation, statistical analysis, drafting of the manuscript; NTA: Data acquisition, clinical and pathological data review, interpretation of results, and critical revision of the manuscript; NCL: Study supervision, methodological guidance, interpretation of findings, and critical revision of the manuscript; LVK: Data collection, imaging assessment, and manuscript review; NNT: Data acquisition, literature review, and manuscript editing; VLM: Statistical support, data interpretation, and manuscript editing; NHH: Clinical coordination, data curation, and manuscript review; VDL: Conceptualization, overall supervision, critical revision of the manuscript, and final approval of the version to be submitted. All authors read and approved the final manuscript.

**Funding:** This research received no external funding.

**Institutional Review Board Statement:** This study was conducted in accordance with the Declaration of Helsinki and was approved by the Biomedical Ethics Committee of Bach Mai Hospital (Code: IRB00009695; Date: 24 April 2025). Patients and their families were thoroughly informed about the study objectives and procedures. Participants were free to withdraw from the study at any time.

**Informed Consent Statement:** Informed consent was obtained from all subjects involved in the study.

**Data Availability Statement:** The data presented in this study are available from the corresponding author on reasonable request. The data are not publicly available because they contain potentially identifiable clinical information.

**Acknowledgments:** The authors thank the staff of Bach Mai Hospital and K Hospital for their support in patient recruitment, imaging acquisition, and pathological assessment.

**Conflicts of Interest:** The authors declare no conflicts of interest.

## References

1. Bray F, Laversanne M, Sung H, et al. Global cancer statistics 2022: GLOBOCAN estimates of incidence and mortality worldwide for 36 cancers in 185 countries. *CA: a cancer journal for clinicians*. May-Jun 2024;74(3):229-263. doi:10.3322/caac.21834
2. Huy Do S. Epidemiology of Hepatitis B and C Virus Infections and Liver Cancer in Vietnam. *Euroasian journal of hepato-gastroenterology*. Jan-Jun 2015;5(1):49-51. doi:10.5005/jp-journals-10018-1130
3. Martins-Filho SN, Paiva C, Azevedo RS, Alves VAF. Histological Grading of Hepatocellular Carcinoma-A Systematic Review of Literature. *Frontiers in medicine*. 2017;4:193. doi:10.3389/fmed.2017.00193
4. Edmondson HA, Steiner PE. Primary carcinoma of the liver: a study of 100 cases among 48,900 necropsies. *Cancer*. May 1954;7(3):462-503. doi:10.1002/1097-0142(195405)7:3<462::aid-cnrcr2820070308>3.0.co;2-e
5. Rodríguez-Perálvarez M, Luong TV, Andreana L, Meyer T, Dhillon AP, Burroughs AK. A systematic review of microvascular invasion in hepatocellular carcinoma: diagnostic and prognostic variability. *Annals of surgical oncology*. Jan 2013;20(1):325-39. doi:10.1245/s10434-012-2513-1
6. Van Beers BE, Pastor CM, Hussain HK. Primovist, Eovist: what to expect? *Journal of hepatology*. Aug 2012;57(2):421-9. doi:10.1016/j.jhep.2012.01.031
7. Kitao A, Matsui O, Yoneda N, et al. The uptake transporter OATP8 expression decreases during multistep hepatocarcinogenesis: correlation with gadoxetic acid enhanced MR imaging. *European radiology*. Oct 2011;21(10):2056-66. doi:10.1007/s00330-011-2165-8
8. Lee S, Kim SH, Lee JE, Sinn DH, Park CK. Preoperative gadoxetic acid-enhanced MRI for predicting microvascular invasion in patients with single hepatocellular carcinoma. *Journal of hepatology*. Sep 2017;67(3):526-534. doi:10.1016/j.jhep.2017.04.024
9. Zhou Z, Cao S, Chen C, et al. A Novel Nomogram for the Preoperative Prediction of Edmondson-Steiner Grade III-IV in Hepatocellular Carcinoma Patients. *Journal of hepatocellular carcinoma*. 2023;10:1399-1409. doi:10.2147/jhc.s417878
10. Samban SS, Hari A, Nair B, et al. An Insight Into the Role of Alpha-Fetoprotein (AFP) in the Development and Progression of Hepatocellular Carcinoma. *Molecular biotechnology*. Oct 2024;66(10):2697-2709. doi:10.1007/s12033-023-00890-0
11. Demirtas CO, D'Alessio A, Rimassa L, Sharma R, Pinato DJ. ALBI grade: Evidence for an improved model for liver functional estimation in patients with hepatocellular carcinoma. *JHEP reports : innovation in hepatology*. Oct 2021;3(5):100347. doi:10.1016/j.jhepr.2021.100347
12. Choi JY, Lee JM, Sirlin CB. CT and MR imaging diagnosis and staging of hepatocellular carcinoma: part II. Extracellular agents, hepatobiliary agents, and ancillary imaging features. *Radiology*. Oct 2014;273(1):30-50. doi:10.1148/radiol.14132362
13. Chernyak V, Fowler KJ, Kamaya A, et al. Liver Imaging Reporting and Data System (LI-RADS) Version 2018: Imaging of Hepatocellular Carcinoma in At-Risk Patients. *Radiology*. Dec 2018;289(3):816-830. doi:10.1148/radiol.2018181494
14. Ahn SY, Lee JM, Joo I, et al. Prediction of microvascular invasion of hepatocellular carcinoma using gadoxetic acid-enhanced MR and (18)F-FDG PET/CT. *Abdominal imaging*. Apr 2015;40(4):843-51. doi:10.1007/s00261-014-0256-0
15. Kim KA, Kim MJ, Jeon HM, et al. Prediction of microvascular invasion of hepatocellular carcinoma: usefulness of peritumoral hypointensity seen on gadoxetate disodium-enhanced hepatobiliary phase images. *Journal of magnetic resonance imaging : JMRI*. Mar 2012;35(3):629-34. doi:10.1002/jmri.22876
16. Bai DS, Zhang C, Chen P, Jin SJ, Jiang GQ. The prognostic correlation of AFP level at diagnosis with pathological grade, progression, and survival of patients with hepatocellular carcinoma. *Scientific reports*. Oct 9 2017;7(1):12870. doi:10.1038/s41598-017-12834-1
17. Edoon MIA, Chutturghoon VK, Wusu-Ansah GK, et al. Serum Biomarkers AFP, CEA and CA19-9 Combined Detection for Early Diagnosis of Hepatocellular Carcinoma. *Iranian journal of public health*. Feb 2019;48(2):314-322.
18. Yan Y, Si Z, Chun C, et al. Multiphase MRI-Based Radiomics for Predicting Histological Grade of Hepatocellular Carcinoma. *Journal of magnetic resonance imaging : JMRI*. Nov 2024;60(5):2117-2127. doi:10.1002/jmri.29289

19. Mao Y, Wang J, Zhu Y, et al. Gd-EOB-DTPA-enhanced MRI radiomic features for predicting histological grade of hepatocellular carcinoma. *Hepatobiliary surgery and nutrition*. Feb 2022;11(1):13-24. doi:10.21037/hbsn-19-870
20. He H, Li X, Liu J, et al. The Combination of Gd-EOB-DTPA Enhanced T1 Mapping with Apparent Diffusion Coefficient could Improve the Diagnostic Efficacy of Hepatocellular Carcinoma Grading. *Current medical imaging*. 2024;20:e15734056259418. doi:10.2174/0115734056259418231112102249
21. Zhao H, Chen C, Gu S, et al. Anatomical versus non-anatomical resection for solitary hepatocellular carcinoma without macroscopic vascular invasion: A propensity score matching analysis. *Journal of Gastroenterology and Hepatology*. 2017/04/01 2017;32(4):870-878. doi:https://doi.org/10.1111/jgh.13603
22. Qin S, Chen M, Cheng AL, et al. Atezolizumab plus bevacizumab versus active surveillance in patients with resected or ablated high-risk hepatocellular carcinoma (IMbrave050): a randomised, open-label, multicentre, phase 3 trial. *Lancet (London, England)*. Nov 18 2023;402(10415):1835-1847. doi:10.1016/s0140-6736(23)01796-8

**Disclaimer/Publisher's Note:** The statements, opinions and data contained in all publications are solely those of the individual author(s) and contributor(s) and not of MDPI and/or the editor(s). MDPI and/or the editor(s) disclaim responsibility for any injury to people or property resulting from any ideas, methods, instructions or products referred to in the content.